Materials & Design 257 (2025) 114459

Contents lists available at ScienceDirect

Materials & Design

journal homepage: www.elsevier.com/locate/matdes

Optimizing foamed glass production with machine learning

Uroš Hribar [a,*], Sintija Stevanoska [a,b], Christian L. Camacho-Villalón [a,c], Matjaž Spreitzer [a], Jakob König [a,1], Sašo Džeroski [a,b,1]

[a] Jožef Stefan Institute, Jamova cesta 39, Ljubljana, 1000, Slovenia
[b] Jožef Stefan International Postgraduate School, Jamova cesta 39, Ljubljana, 1000, Slovenia
[c] IRIDIA, Université Libre de Bruxelles, Av. Franklin Roosevelt 50, Brussels, 1050, Belgium

ARTICLE INFO

Dataset link: 10.5281/zenodo.15023205, https://github.com/sintija-s/foaming-glass

Keywords:
Foamed glass
Machine learning
Process optimization
Waste glass

ABSTRACT

Foamed glass is a lightweight material commonly used for insulation. However, optimizing its properties remains a challenge due to the large number of synthesis parameters involved in its production. While previous studies have investigated synthesis conditions, a comprehensive study applying machine learning approaches is lacking in the literature. In this paper, we apply machine learning methods, i.e., random forests of predictive clustering trees and a multilayer perceptron, training them on 124 experimental data points to accurately predict the apparent density and closed porosity of foamed glass. We then apply a multiobjective optimization algorithm together with the multilayer perceptron to find optimal values for the process parameters used in foamed glass production. Our results show that the combination of machine learning and multiobjective optimization is an effective proxy for the development of novel foamed glass materials.

1. Introduction

Foamed glass is a versatile material that has received considerable attention in research and development over the past few years. Its cellular structure, characterized by sealed pores, offers a range of desirable properties including low density, excellent thermal insulation, moisture resistance, fire resistance, and high compressive strength. These attributes make foamed glass a compelling subject for scientific research in construction, insulation, and environmental remediation. Furthermore, foamed glass presents a promising solution for the management of specific waste streams that would otherwise be relegated to landfills, fostering waste reduction and promoting a circular economy.

Indeed, sustainability is an important aspect in materials optimization, especially when it comes to construction materials, considering that 40% of the energy consumed in the European Union is used in buildings and 80% from that goes into heating and cooling [1]. The measures to increase the average energy performance of residential buildings by 16% by 2030 (compared to 2020) and the enhanced standards that require calculating the whole-life-cycle carbon emissions of new buildings demonstrate that, aside from performance, improved sustainability is essential when developing or optimizing construction insulation materials. Improving methods to adjust glass composition through re-melting and the use of a special furnace atmosphere can result in foamed glass with significantly improved properties [2]. However, scientific and commercial developments of foamed glass emphasizing sustainable aspects have shown that high-performance materials can be developed without the use of energy-intensive re-melting of waste glass.

Several studies have explored the use of various waste glass compositions for foamed glass production, which promotes sustainable development while potentially facilitating a reduction in the cost of foamed glass. Sources of waste glass investigated for foamed glass production include flat glass [3], container glass [4], waste glass derived from automotive vehicles [5], and E-glass [6]. Additionally, several waste by-products generated during large-scale industrial processes, such as red mud [7], lime mud [8], aluminum dross [9], fly ash [10], slags [11,12], as well as natural materials like eggshells [13], oyster shells [14], rice husk and pine scales [15] are being studied as potential additives in the synthesis of foamed glass. However, the outcomes of previous studies are often specific to the exact composition used, limiting their broader applicability. Consequently, alternative approaches have been proposed to discover new foaming compositions that result in foamed glass with favorable performance characteristics [16]. One

* Corresponding author.
E-mail addresses: uros.hribar@ijs.si (U. Hribar), sintija.stevanoska@ijs.si (S. Stevanoska), ccamacho@ulb.ac.be (C.L. Camacho-Villalón), matjaz.spreitzer@ijs.si (M. Spreitzer), jakob.konig@ijs.si (J. König), saso.dzeroski@ijs.si (S. Džeroski).
[1] Joint last authors.

https://doi.org/10.1016/j.matdes.2025.114459
Received 21 March 2025; Received in revised form 27 June 2025; Accepted 23 July 2025

Available online 30 July 2025

of these approaches consists modeling the process at the level of basic physical phenomena—sintering, gas evolution, formation of bubbles, and their growth. However, this approach can only leverage a limited amount of data on glass properties at foaming temperatures and has high computational costs due to the need to simulate the complex dynamic of bubble formation, stability, and growth even in small systems.

On the other hand, with a sufficient amount of experimental data, a machine learning approach could present an alternative avenue for describing the outcome of the foaming process based on the input parameters. Such an approach has the potential to significantly reduce the computational burden associated with modeling while offering additional insights into the correlations between the process parameters and material properties [17,18]. Furthermore, by implementing the aforementioned approach and leveraging insights derived from a diverse range of waste glass compositions and foaming additives, it is possible to generate recommendations for optimal compositions of waste glass that have not been previously explored. Prior to such a large-scale study, an initial investigation is imperative to assess the feasibility and applicability of the described approach.

The system comprising cathode-ray-tube (CRT) panel glass, carbon, and manganese oxide has been extensively studied in the past [19]. It is well established that manganese oxide, at elevated temperatures, releases additional oxygen, which promotes the reaction with carbon, leading to the formation of carbon dioxide. This process is shown in Equation (1) as follows:

$$Mn_3O_4 + \frac{1}{2}C \longrightarrow 3MnO + \frac{1}{2}CO_2 \quad (1)$$

From a sustainable development perspective, it is energetically advantageous to use simple processing methods without the need to control the furnace atmosphere [20]. However, applying the manganese–carbon reaction in an air atmosphere typically leads to premature oxidation of carbon, resulting in poor expansion. In this context, the use of water glass becomes essential. By protecting the carbon component, water glass enables the effective use of the manganese–carbon system even in the presence of air [21]. Although the introduction of water glass adds complexity to the system, CRT panel glass remains an ideal model material for early-stage research due to its high stability against crystallization. This makes it particularly suitable for initial model development.

In recent years, machine learning (ML) has become an increasingly important tool in materials science, enabling data-driven insights that would be difficult to obtain through traditional experimentation or simulation alone. In particular, supervised learning methods have been used to model complex, non-linear relationships between processing parameters and material properties, often improving prediction accuracy and accelerating materials design pipelines [22,23].

In this paper, we establish a data-driven framework for optimizing the properties of foamed glass, facilitating precise control over its structural properties using ML and multiobjective optimization. In particular, we use two ML techniques well-suited for multi-target regression problems. First, we investigate the importance and effect of the process parameters on foamed glass properties, using a data set of 124 foamed glass samples. Second, we predict the values of the characterization parameters beyond the range of the foamed glass samples in the data set. Finally, we incorporate a multiobjective optimization algorithm, which searches for optimal process parameters while accounting for model uncertainty, a crucial aspect in high-stakes applications such as materials synthesis. Our ML framework offers two main contributions for foamed glass production research: (i)interpretability of the results and identification of the key process parameters, and (ii) extrapolation of the considered data set to reveal new process parameter combinations.

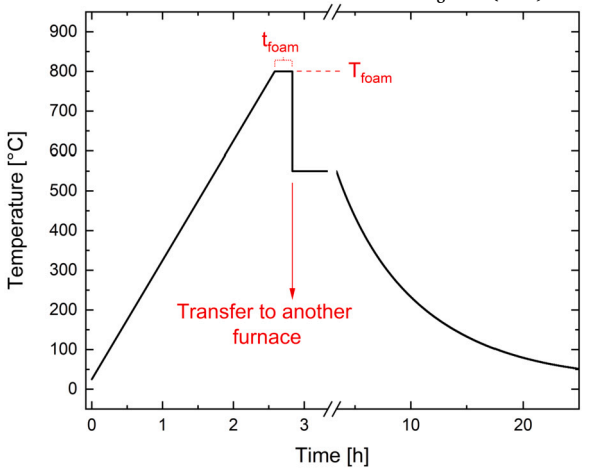

Fig. 1. Temperature-time profile used for the thermal treatment.

2. Methods

2.1. Foamed glass preparation

Raw waste CRT panel glass powder, used as the main component for the preparation of foamed glass samples, was provided by Averhof A/S (Aarhus, Denmark). The mean particle size of the received glass powder was approximately 13 μm. The chemical composition of CRT panel glass is shown in Table 1.

Different amounts of potassium phosphate (K_3PO_4, 98%, Alfa Aesar, Karlsruhe, Germany), carbon (carbon black, Lehman & Voss & Co, Hamburg, Germany) and manganese oxide (Mn_3O_4) were combined with CRT powder for the preparation of the foaming mixtures. Mn_3O_4 was obtained by treating MnO_2 at 1250 °C for 4 h [24]. Note that manganese is present in Mn_3O_4 in two oxidation states and could also be written as $MnO \cdot Mn_3O_4$. Foaming mixtures were milled in a planetary ball mill with 10 mm yttria-stabilized zirconia balls at 250 rpm for 30 min, followed by additional milling (5 min) after the addition of Mn_3O_4. The foaming mixtures were manually combined with various amounts of water glass solution (WG, SiO_2 to Na_2O ratio 1.85 to 1). The values of the process parameters were chosen based on the observations from our previous investigation [21] and are presented below in Table 2.

After the above-described processing, some of the foaming mixtures were additionally homogenized (mixing with a laboratory tumbler for 15 minutes, labeled as “mixing”, in Table 2) and/or dried (at 90 °C for 3 h, labeled as “drying”, in Table 2). Additional mixing of the foaming mixtures using a laboratory tumbler was introduced to assess whether it is necessary to improve the homogenization for this specific foaming process and to evaluate its potential influence on the final properties of the material. The drying step was motivated by the known reactivity between water glass and atmospheric CO_2 [21]. In [21], we showed that mixtures containing glass and water glass begin to react with CO_2 from the air, and that the extent of this reaction can significantly influence the foaming outcome and compromise process repeatability. Since this reaction only continues in the presence of moisture, drying the samples effectively halts further reaction. This allowed us to investigate whether the foaming mixtures are affected by the extended reaction times during the processing.

To obtain initial green pellets with similar dimensions, 1 g of a foaming mixture was pressed in a cylindrical steel die (inner diameter 12 mm) with 3.5 MPa. Pellets were thermally treated in a chamber furnace (BOSIO laboratory chamber furnace with a 20-litre chamber) with a heating rate of 5 °C min^{-1}, starting from the room temperature. The final foaming temperature (T_{foam}) and foaming time (t_{foam}) varied between 700-805 °C and 0-60 min, respectively. After a given t_{foam}, the

Table 1
Chemical composition of CRT glass powder (analysis of X-ray fluorescence) expressed in weight percentages (wt.%). From [19].

	Na_2O	MgO	Al_2O_3	SiO_2	K_2O	CaO	Fe_2O_3	SrO	ZrO_2	BaO
Composition (wt.%)	7.7	0.3	2.4	61.0	7.1	0.8	0.2	7.8	1.5	9.7

Table 2
Overview of process parameters and their values.

Process parameter	Range	Values
WG content (wt.%)	0-30	0, 4, 8, 12, 16, 20, 24, 30
carbon black content (wt.%)	0-0.84	0, 0.42, 0.525, 0.63, 0.84
Mn_3O_4 content (wt.%)	0 – 6.356	0, 6.356
K_3PO_4 content (wt.%)	1 – 4	1, 2, 4
mixing	Yes / No	Yes, No
drying	Yes / No	Yes, No
T_{foam} [°C]	700 – 805	700, 720, 745, 790, 805
t_{foam} [min]	0 – 60	0, 5, 10, 20, 30, 60

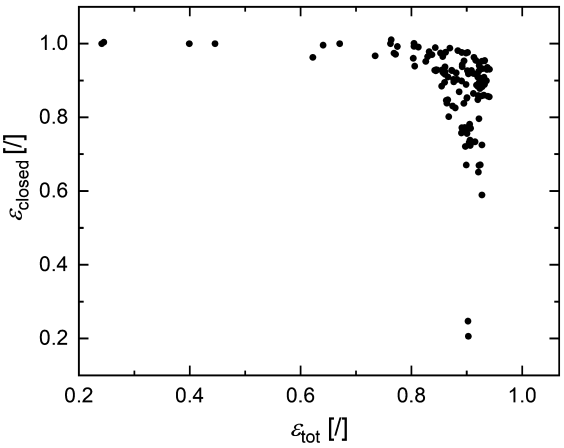

Fig. 2. ε_{closed} versus ρ_{app} distribution of the training dataset.

samples were transferred to another furnace (kept at 550 °C) in order to ensure the freezing of the porous structure. To prevent cracking and enable relaxation of stresses induced during rapid cooling, the samples were kept at 550 °C for an additional 30 min and then allowed to naturally cool inside the furnace (1). The values used for T_{foam} and t_{foam} are given in Table 2.

2.2. Foamed glass characterization

Apparent and pycnometric densities (ρ_{app} and ρ_{pyc}, respectively) of the foamed glass samples were measured using the Archimedes method. The ρ_{app} was determined by weighing the foamed glass sample in distilled H_2O, while the ρ_{pyc} was determined by first submerging the sample in anhydrous ethanol, evacuating it to fill the open pores with ethanol, followed by weighing in the same medium. The density of the received glass (2600 kg m^{-3}) was measured with a gas pycnometer (Ultrapyc 5000 Foam, Anton Paar) and considered as powder density (ρ_{pow}) for the calculation of total (ε_{tot}) and closed porosity (ε_{closed}) of the foamed glass samples according to Equations (2) and (3).

$$\varepsilon_{tot} = 1 - \frac{\rho_{app}}{\rho_{pow}}, \tag{2}$$

$$\varepsilon_{closed} = \left(\frac{1}{\rho_{pyc}} + \frac{1}{\rho_{pow}}\right)\left(\frac{1}{\rho_{app}} + \frac{1}{\rho_{pow}}\right)^{-1}. \tag{3}$$

Fig. 2 presents the data on ε_{tot} and ε_{closed} of all foamed glass samples within the training set. It shows that a wider range of ε_{closed} values is achievable with increasing total porosity, which is consistent with the results reported by König et al. [19]. Achieving high ε_{tot} and ε_{closed} is essential in foamed glass synthesis in order to optimize the thermal insulation, moisture resistance, and mechanical strength of foamed glass. However, a large number of synthesis parameters make it challenging to identify the combination that achieves the desired balance between the processes that occur during foaming. Also, optimizing multiple synthesis parameters simultaneously can be a complex task, since changes in one parameter may have unintended consequences on the others. To address this challenge, machine learning methods can assist in exploring the parameter space and identifying the key factors that affect the properties of interest, i.e. ρ_{app}, and ε_{closed}.

3. Machine learning and optimization methodologies

3.1. Data

The dataset used for training by the machine learning methods consists of 124 foamed glass samples prepared as described in Section 2.1. Each sample is defined as a pair of experimental foamed glass process parameters and its corresponding properties. The experimental parameters listed in Table 2 define the feature space used to train the ML models to predict the target variables—in this case, ρ_{app}, ρ_{pyc}, ε_{tot}, ε_{closed} and ε_{open}, as described in Section 2.2. All variables in the feature and target spaces were treated as continuous, with the exception of mixing and drying, which were treated as binary.

3.2. Machine learning algorithms

We use ML for two tasks. The first task is related to exploring the data and identifying the key experimental parameters. This involves determining which experimental parameters influence the characterization properties the most and making initial predictions for the values of the characterization properties within the observed data ranges. For this first task, we used random forests of predictive clustering trees for multi-target prediction.

The second task is to explore which combination of experimental parameters would yield optimal characterization properties. For this task, we trained a neural network (NN) for multi-target prediction, specifically a multilayer perceptron (MLP), on the available data. The trained MLP was used as an objective function for an optimization algorithm in order to find suitable combinations of experimental parameter values which simultaneously minimize ρ_{app} and maximize ε_{closed}.

3.2.1. Task 1: Importance and the effect of process variables on selected properties

Predictive clustering trees (PCTs) treat a decision tree as a hierarchy of clusters, starting with all data in one group and splitting it into smaller, more compact clusters as the tree grows. The `CLUS` package [25] implements the learning of PCTs, both single trees and ensembles of trees. To decide how to split the data at each step, PCTs use a heuristic that picks the feature that reduces variance the most, ensuring that each new cluster is as homogeneous as possible, thus improving the predictive accuracy of the model. To increase prediction robustness, individual PCTs can be combined into ensembles, such as random forests, of PCTs. In a random forest, as defined by Breiman [26], the prediction for a new example is generated by aggregating the predictions from all the trees within the ensemble. Using ensembles of PCTs, we compute feature importance using the *Genie*3 score. Feature ranking assigns relevance scores that show how much each feature impacts the target. This

score prioritizes features that reduce target impurity the most, giving more weight to splits near the root of the tree.

The task at hand is to predict the five properties of foamed glass (ρ_{app}, ρ_{pyc}, ε_{tot}, ε_{closed} and ε_{open}), from the processing parameters described in Section 2.1. The input data, described in Section 3.1, is used to train a random forest of PCTs, consisting of 100 individual trees. The predictive performance of the ensemble on unseen cases is assessed by measuring the Pearson correlation coefficient through a 10-fold cross-validation. This coefficient measures the strength and direction of the linear relationship between two variables. As a performance metric in a regression problem, the Pearson correlation coefficient measures how strongly the original and the predicted values of the target variables are related. A value close to 1 means a strong positive relationship, a value close to -1 means a strong negative relationship and a value close to 0 means little or no linear relationship. Although some of the five investigated properties are mathematically related and could be derived from one another (Equations (2) and (3)), we chose to include them all as separate targets in the model. This approach allowed us to test the model's ability to predict each parameter independently, even in those cases where the prediction may seem redundant due to simple interdependence.

3.2.2. Task 2: Determination of optimal parameters to achieve a desired composition

The goal of the second task is to train a model that can be used as an objective function for an optimization algorithm in order to obtain process parameters that yield low ρ_{app} and high ε_{closed}. This cannot be effectively done using random forests of PCTs, since they are constrained to predict values only within the observed training data range and struggle with extrapolation. To overcome this limitation, we trained an MLP for the second task, which is a NN-based approach better suited for extrapolation, i.e., for making predictions beyond the range of the observed data.

The MLP has a simple architecture consisting of three linear layers activated by ReLU, using the Smooth L_1 as the loss function. Since we are not only interested in the predictions, but also in the model's uncertainty in the prediction, we measure the performance of the model aggregated across 10 runs with different random weight initializations. Then, we computed the semi-deviation of the predictions over 10 runs and used it as a parameter in the optimization algorithm to penalize solutions that might yield worse results than predicted.

3.3. Multiobjective optimization

We use a multiobjective optimization approach to find combinations of process parameters that lead to desired characterization values (ρ_{app}, ε_{closed}) for the foaming process. In a multiobjective optimization problem, instead of searching for a single solution that optimizes all objectives simultaneously, we search for a set of solutions that provide the best trade-off between the objectives. In practice, an optimal solution to a multiobjective optimization problem (referred to as a non-dominated solution or as a Pareto-optimal solution) is one for which it is not possible to improve on one objective without worsening on the others [27,28]. In this study, our goal is to find Pareto-optimal solutions to design foamed glass; in other words, we are looking for the set of process parameter values that result in the lowest ρ_{app} for a given closed porosity, or in the highest ε_{closed} for a given apparent density.

We implemented the Indicator-Based Evolutionary Algorithm [28] (IBEA) using the ParadisEO software framework [29]. IBEA is a multiobjective evolutionary algorithm, in which a population of solutions (or individuals) are handled simultaneously to perform a parallel exploration of the search space. The population is evolved in order to get it both as close as possible to the Pareto-optimal set and uniformly distributed. The evolution process is done by the iterative application of four operators: parental selection, which specifies which individuals are selected from the population to produce new solutions; crossover and mutation, which create new solutions and apply small changes to them; and survival selection, to discard low-quality solutions.

The parameters of IBEA were set as follows: the maximum number of generations is 10000, the crossover probability is 1.0, and the mutation rate is 0.083. Also, as mentioned in Section 3.2.2, we use the semi-deviation of the predicted values as a parameter in our implementation to penalize solutions based on their uncertainty. The semi-deviation is a dispersion measurement that takes into account only values below the predicted mean, but not those above it, thus making it appropriate to quantify possible losses without penalizing possible gains. In practice, in our implementation of IBEA, the quality of a solution is computed as the following weighted sum $(0.9 * sol) + (0.1 * sol * sdv)$, where sol is the value predicted by the MLP for a particular characterization parameters vector, and sdv is the semi-deviation of the characterization parameters vector computed across 10 independent runs of the MLP using different random weight initializations. Therefore, the larger the semi-deviation of the solution, the more the solution is penalized.

4. Results and discussion

4.1. Importance and the effect of process variables on selected properties

For this part of the study, we trained a random forest of 100 PCTs, achieving a highly accurate match between the actual and predicted values of ρ_{app}. Namely, we measured a Pearson correlation coefficient of 0.96. For comparison, we also applied linear regression to the same dataset, and for the same target variable we achieved a significantly lower Pearson correlation coefficient of 0.72. Note that these figures refer to predictions on data not used during training. To ensure a reliable evaluation, we used 10-fold cross-validation approach. In this approach, the data is split into 10 equal parts, and the model is trained 10 times, each time using 9 parts for training and the remaining part for testing. The reported performance is the average over these 10 test runs.

4.1.1. Process variable importance

From the process parameter variables, we predicted five foamed glass properties: ρ_{app}, ρ_{pyc}, ε_{tot}, ε_{closed} and ε_{open}. The overall importance of individual variables in predicting all material properties, along with their specific importance for each individual material property, is evaluated using random forests of PCTs (Section 3.2.1). In Table 3, we show the rankings assigned to the process parameter variables, where lower values for the ranking indicate higher importance. The WG content parameter stands out as the most important, both in general and individually for each investigated property. It is known that WG significantly affects the sintering and expansion behavior of the foaming mixture, enabling the reaction between Mn_3O_4 and carbon black in the air atmosphere [30], while also directly contributing to foaming [21]. The content of WG thus affects the process dynamics at multiple levels, making it likely that the model identifies WG content as the most critical variable.

The contents of carbon black and Mn_3O_4 were evaluated as the second or third most important parameters in general and for each measured material property (Table 3). Furthermore, the model attributes similar significance to both parameters, which is highly likely to be associated with the actual phenomena occurring during the foaming process.

The importance of drying, mixing, and K_3PO_4 content is evaluated as very low, being ranked either sixth, seventh or eighth for all material properties, with one exception related to the importance of K_3PO_4 content for ε_{closed} (Fig. 3 and Table 3). These results are evidence of the predictive capabilities of the model, since K_3PO_4 is added solely for its impact on the characteristic temperatures of glass [31], which affects the pore structure, and consequently, the value of ε_{closed}.

The model estimates that T_{foam} has a greater influence on ε_{closed} than on ε_{tot} (Fig. 3 and Table 3). This result can be correlated with a previously observed phenomenon, where the change of T_{foam} results only in a

Table 3
Parameters ranked by their importance with respect to the overall outcome (all material properties) and with respect to a specific material property.

Parameters	Overall	ρ_{app}	ρ_{pyc}	ε_{tot}	ε_{closed}
WG content	1	1	1	1	1
carbon black content	2	3	2	3	3
Mn_3O_4 content	3	2	3	2	4
K_3PO_4 content	7	8	7	8	5*
mixing	8	7	8	7	8
drying	6	6	6	6	7
T_{foam}	4	4	4	4	2
t_{foam}	5	5	5	5	6

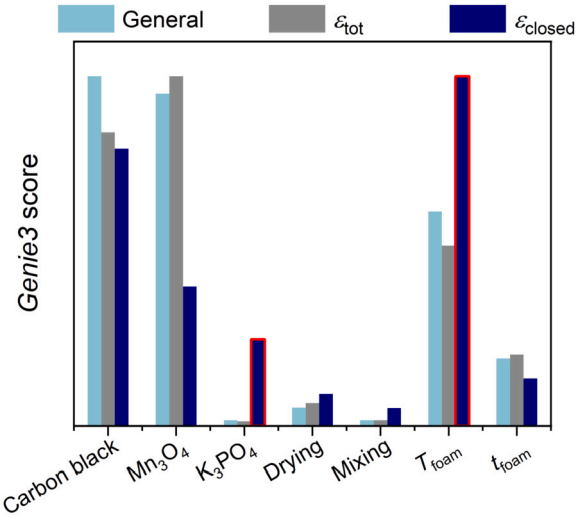

Fig. 3. The importance (*Genie3* score) of process parameters (excluding the content of WG parameter), with respect to their overall importance for the five properties, as well as their importance for ε_{tot} and ε_{closed}.

slight change of the ε_{tot}, while the content of ε_{closed} can change dramatically. The increase of ε_{tot} at low T_{foam} values is usually related to the nucleation of new pores, while it becomes more related to pore growth at high T_{foam} values [32]. Larger pores further promote pore merging (coalescence), which leads to inhomogeneous pore size distribution, abnormally large pores, and open porosity and eventually results in a foam with poor mechanical stability. This phenomenon suggests that at high T_{foam} values, the kinetics of pore opening will be significantly faster in comparison to pore growth and foam expansion. Note that the majority of the samples in this research (training set) exhibit high total porosity values (Fig. 2).

Interestingly, the model does not recognize the effect of t_{foam} on ε_{closed}. Prolonged t_{foam} often results in larger and also more open pores (lower ε_{closed}). The training dataset encompasses a broad range of t_{foam} values, providing the opportunity for this effect to occur. However, it can be noticed that higher t_{foam} values were commonly used in combination with relatively low T_{foam}. This combination of parameters could require even longer t_{foam} for the observable effects of coalescence to manifest, explaining the model's evaluation in this case.

4.1.2. Prediction of new compositions

The random forest of PCTs model was further used to predict the properties of several compositions with process parameters within the range of the training set (Table 4). Since drying, mixing, and t_{foam} were evaluated as the least important parameters in the first part of the study, they were not varied in the following predictions. The model was also used to predict the effect of certain parameters on the predicted properties. The values of the parameters presented in Table 4 were chosen particularly to investigate the influence of K_3PO_4, Mn_3O_4, carbon black, and WG in a new composition. Data generated from the first and second parameter sets is shown in Fig. 4 and Fig. 5, respectively.

Table 4
Values for the process parameters used to predict the properties of glass foams for the evaluation of the model accuracy.

Process parameter	Parameter set no.1	Parameter set no.2
WG content [wt.%]	4, 8, 12	0-30 with step 1
carbon black content [wt.%]	0.4, 0.6, 0.84	0, 0.06
Mn_3O_4 content [wt.%]	0, 2, 4	0, 2
K_3PO_4 content [wt.%]	4, 6, 8	2
drying	No	No
mixing	No	No
T_{foam} [°C]	770-840 with 10 °C steps	700, 790, 850
t_{foam} [min]	2, 4, 6, 8	5

An increase of ε_{tot} can be achieved with higher content of WG as shown in Fig. 4a. The model predicts that low contents of WG result in low ε_{tot} and high ε_{closed}, which is in agreement with the experimental results. Implementation of carbon black as a foaming agent in the air atmosphere is not suitable due to the premature combustion of carbon black in reaction with oxygen [33]. The application of WG retards this reaction and enhances the foaming [21]. The model further predicts that the range of achievable ε_{closed} widens significantly with higher content of WG, which is also expected since interconnected pores in foamed glasses are more likely to form at higher ε_{tot} values. The content of interconnected pores is an important material characteristic, which significantly affects the properties and applicability of the material. Control over the ε_{closed} in foamed glass, especially in high ε_{tot} regions, can be extremely difficult since it depends on several factors [19]. However, a fairly high ε_{closed} value at higher ε_{tot} values can only be achieved with higher contents of K_3PO_4, as evidenced from the Fig. 4b. Such characteristic (high ε_{tot} and ε_{closed}) is of practical importance, since it normally results in lower thermal conductivity while keeping the material water-impermeable. No clear trend on the ratio between ε_{tot} and ε_{closed} was observed from the model predictions for other investigated parameters. The effect of prolonged t_{foam} is commonly researched, and while it can result in higher ε_{tot}, it almost always also results in a decreased ε_{closed} [14].

The predictions generated for the parameter set no.2 in Table 4 reveal how various combinations of additives are expected to affect the outcome of the foaming process (Fig. 5). The formation of CO_2, and its consequential influence on expansion, requires the presence of both carbon black and Mn_3O_4 [30,33]. Therefore, the influence of either carbon black or Mn_3O_4 becomes evident only when a reaction between them can occur, i.e., when the content of neither of them is 0. As already seen from the evaluation of the parameter importance (Table 3), the model evaluates that the impact of carbon black and Mn_3O_4 on the process is similar, which is reasonable since, in reality, neither of the additives affects the process significantly on its own. Additionally, the expansion values predicted from Table 4, shown in Fig. 5, confirm that the model is capable of identifying the role of the additives, such as Mn_3O_4, carbon black, and WG.

An increase in WG content leads to greater expansion value of newly proposed compositions, even when the content of carbon black and Mn_3O_4 is zero (data labeled "None" in Fig. 5), which corresponds to direct contribution of WG [21]. Here, it should be mentioned that, in reality, the observed change in the expansion with increasing WG content is more continuous than predicted by the model in Fig. 5. The step-like dependence of expansion (ε_{tot}) in Fig. 5 can be explained based on the training dataset. The actual WG content values within the training dataset are in the same range as in Fig. 5, however, the increment of WG content in the training dataset was approximately 4. It is likely that examples with similar WG values fall into the same prediction bracket and the model consequently assigns the same value to all the examples within the bracket. The role of Mn_3O_4 and carbon black in the foaming process is to react, produce CO_2, and enable further expansion of

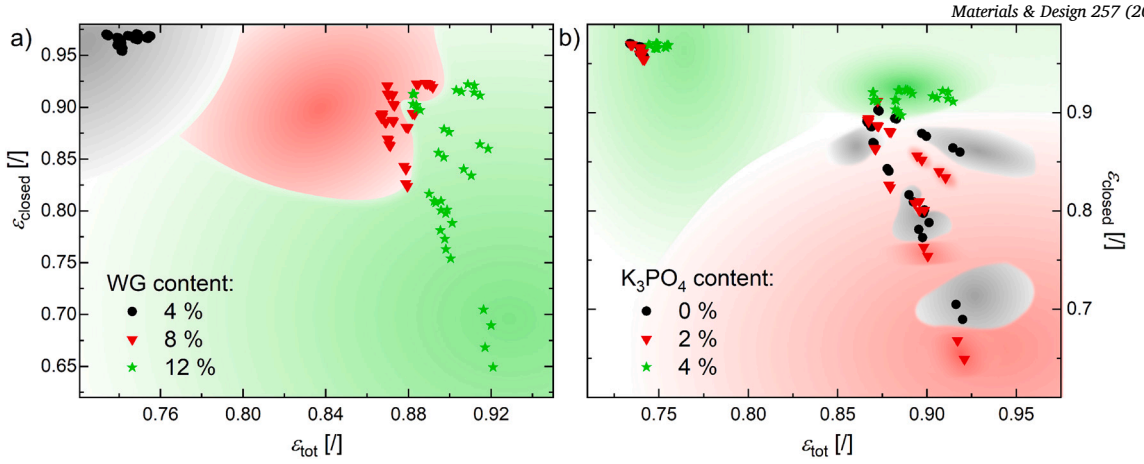

Fig. 4. Values of ε_{closed} versus ε_{tot} predicted for foamed glass samples generated using parameter set no.1 from Table 4, with colored regions corresponding to the content of WG (a) or K_3PO_4 (b).

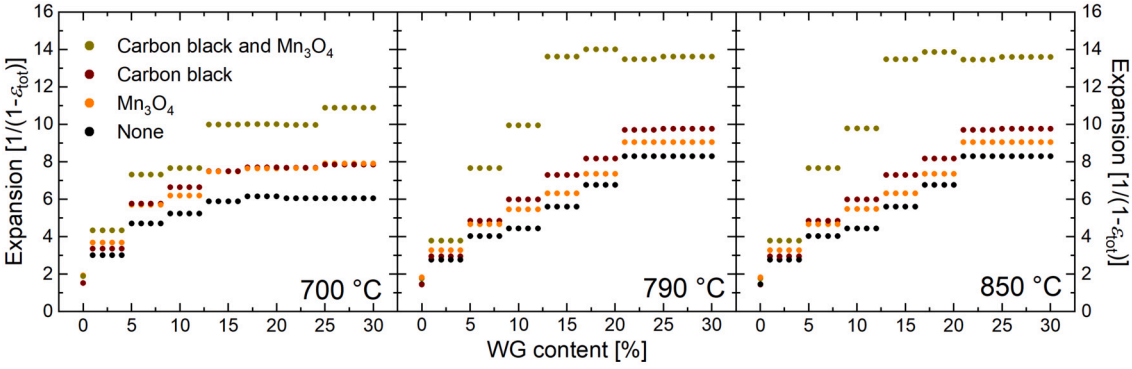

Fig. 5. Predicted expansion values for foamed glass samples that would be synthesized based on parameter set no.2 from Table 4.

the foam. It is therefore expected that expansion values do not change significantly when only one component of a foaming couple is used, i.e. composition contains either only carbon black or only Mn_3O_4 (labeled "Carbon black" and "Mn_3O_4" in Fig. 5). The predictions made by the model shown in Fig. 5 clearly illustrate this fact, where the expansion values of the samples labeled "None", "Mn_3O_4" and "Carbon black" do not vary significantly at the same content of WG. Samples that contain both additives, labeled "Carbon black and Mn_3O_4", expand significantly more in comparison to the other three, confirming the theoretical background, as well as the experimental evaluation.

In terms of temperature dependence, a significant change is expected in the expansion values within the selected temperature range. The comparison between the results in Fig. 5 suggests the opposite. As already mentioned above, the predictive power of the random forest of PCTs depends heavily on the data it takes as input. Due to the lack of examples where T_{foam} is above 805 °C, the model conforms to previously learned rules.

4.2. Finding optimal compositions and experimental validation

In order to predict the properties of process parameters outside of the training set range, we build an MLP and use it in combination with the multiobjective optimization algorithm IBEA (Section 3.3). To obtain a robust estimate of performance, the MLP was trained using 5 different random seeds, which influenced both weight initialization and dataset splits. The final performance is reported as the average Pearson Correlation Coefficient over these runs. The model achieved Pearson correlation coefficients of 0.75 for ρ_{app} and 0.58 for ε_{closed}. The formulation of the optimization problem tackled by IBEA considers two objectives, minimizing the value of ρ_{app} and maximizing the value ε_{closed}, both of which

Table 5
Three sets of parameters and properties selected for further laboratory testing, obtained by the IBEA model.

Process parameter	ML1	ML2	ML3
WG content [wt.%]	30	30	30
carbon black content [wt.%]	1.00	1.00	1.00
Mn_3O_4 content [wt.%]	7.00	7.00	5.29
K_3PO_4 content [wt.%]	4.00	4.00	4.00
drying	No	No	No
mixing	Yes	Yes	Yes
T_{foam} [°C]	800	730	700
t_{foam} [min]	5	5	5
ρ_{app} [kg m^{-3}]	129	162	199
ε_{tot} [%]	95.0	93.8	92.3
ε_{closed} [%]	92	95	97

are desired properties in foamed glass for thermal insulation. Three sets of process parameters suggested by IBEA were chosen and tested in the laboratory by synthesizing the corresponding foamed glasses to further assess the model accuracy. The combinations of parameters and predicted properties are shown in Table 5. Note that the ε_{tot} values were not predicted by the model but calculated from the predicted ρ_{app} values according to Equation (2).

IBEA with ε_{tot} and ε_{closed} set as optimization objectives, yields the results shown in Fig. 6. Three samples were prepared for each chosen set of parameters. In terms of ε_{tot}, the accuracy of the model predictions varies with T_{foam}. For the ML1 and ML2 set of parameters (T_{foam} of 800 and 730 °C) the ε_{tot} predictions agree fairly well with experimental results, on average differing by 1.5%, which is within the predicted uncertainty. At T_{foam} 700 °C (ML3), this difference increases above the predicted uncertainty to 6%. In terms of ε_{closed}, the model predictions

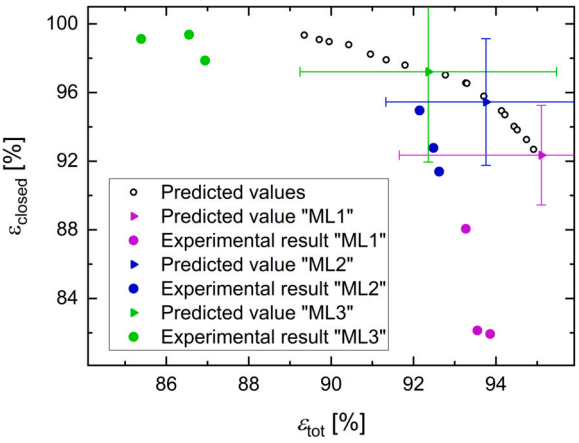

Fig. 6. IBEA predictions (empty black circles) with selected points (closed triangles) and prediction uncertainty (error bars). Corresponding values from additional tests are represented with closed circles.

are more accurate for low ε_{tot} values and increase significantly with increasing ε_{tot}. The ε_{tot} values are within the predicted uncertainty, in the case of ML2 and ML3 parameter combinations, and outside the predicted uncertainty, in the case of ML1. Interestingly, all experimental values fall below the predicted values which could be related to the model's underestimation of the T_{foam} effect. While T_{foam} was evaluated as the most influential parameter, the model still underestimates the impact of decreasing the T_{foam} from 800 to 730 °C on the total porosity.

The lowest average ρ_{app} achieved by following the results obtained by IBEA was 165 kg m^{-3} (equal to ε_{tot} of 93.6%) which is higher when compared to the best commercial waste-based foamed glass products for thermal insulation. Furthermore, the average corresponding ε_{closed} was 84% which suggests that the nature of porosity in the foam is not completely closed. Low ε_{closed} values can affect the material's insulation performance and limit its applicability, as it becomes unsuitable for outdoor use in environments subjected to freeze-thaw cycles. When compared to the properties of the samples from the training set, IBEA was effective at predicting parameter combinations which resulted in high values in both optimized parameters (ε_{closed} and ε_{tot}). For the synthesis of foamed glass improved properties, achieving high ε_{tot} combined with high content of ε_{closed} is crucial. The ability to predict new parameter combinations that lead to such properties can be of significant importance for material optimization.

5. Conclusions

The predictive model for ε_{total}, based on the random forest method, exhibits a strong correlation between the predicted and actual values from the training dataset (0.96). The model's insights into the significance of individual parameters on specific characteristics of foamed glass align well with the findings in the literature on foamed glass. However, further analysis revealed that despite identifying the importance of certain parameters, the random forest of PCTs inadequately estimates the influence of certain variables on material properties. This limitation stems from these parameters being underrepresented or insufficiently varied in the data, leading to the model's inability to extrapolate effectively. When predictions are made for samples with properties that extend beyond or approach the limits of the training set—such as unusually high total or closed porosity—the model's reliability naturally decreases. This highlights a common limitation of data-driven models, where performance tends to decline when extrapolating beyond the domain of the training data. Nevertheless, the properties of the samples synthesized according to the newly predicted compositions are in the top fraction in comparison to the training dataset when it comes to total and closed porosity.

Training an MLP and using its predictions with an optimization algorithm allowed us to obtain several sets of optimal processing parameters when optimizing for low ρ_{app} and high ε_{closed}. The predictions of the model, along with the uncertainty, were used as input to the multiobjective optimization algorithm, which yielded a set of optimal solutions, from which several were chosen to be tested in the laboratory. The tests revealed that the prediction capability of the MLP with the optimization approach yields adequate predictions, even when the predicted material property values are outside their training set range, meaning that the second approach extrapolates successfully. Furthermore, the comparison between the properties of the samples from the training set and newly synthesized samples based on the solutions from the optimization algorithm reveals that the model was able to predict points with optimized values in both parameters (ρ_{app} and ε_{closed}). The data-driven approach proposed in this paper can significantly accelerate the optimization process, reducing the need for extensive trial-and-error experimentation.

CRediT authorship contribution statement

Uroš Hribar: Writing – review & editing, Writing – original draft, Visualization, Validation, Methodology, Investigation, Formal analysis, Data curation. **Sintija Stevanoska:** Writing – review & editing, Writing – original draft, Visualization, Validation, Software, Methodology, Investigation. **Christian L. Camacho-Villalón:** Writing – review & editing, Writing – original draft, Visualization, Validation, Software, Methodology, Investigation, Data curation. **Matjaž Spreitzer:** Writing – review & editing, Validation, Supervision, Resources, Funding acquisition. **Jakob König:** Writing – review & editing, Validation, Supervision, Resources, Methodology, Funding acquisition, Conceptualization. **Sašo Džeroski:** Writing – review & editing, Supervision, Software, Resources, Funding acquisition, Conceptualization.

Declaration of competing interest

The authors declare that they have no known competing financial interests or personal relationships that could have appeared to influence the work reported in this paper.

Acknowledgements

This work was supported by The Slovenian Research and Innovation Agency (ARIS)) via two research programs, Grant numbers P2-0091 and P2-0103 (providing a young researcher grant to Sintija Stevanoska), and three research projects, Grants GC-0001, J7-4636, and J7-4637. It was also supported in part by the EC via the Horizon Europe project ELIAS, Grant 101120237. This publication is supported by the European Union's Horizon Europe research and innovation programme under the Marie Skłodowska-Curie Postdoctoral Fellowship Programme, SMASH co-funded under the grant agreement No. 101081355. The operation (SMASH project) is co-funded by the Republic of Slovenia and the European Union from the European Regional Development Fund.

Data availability

The dataset from this study is available at https://doi.org/10.5281/zenodo.15023205. The code implementation for Task 2 and the multiobjective optimization algorithm (IBEA) are available at https://github.com/sintija-s/foaming-glass.

References

[1] European Parliament and Council of the European Union, Directive (EU) 2024/1275 of the European Parliament and of the Council of 24 April 2024 on the Energy Performance of Buildings (Recast) (Text with EEA Relevance), Off. J. Eur. Union L2024/1275 (May 2024), http://data.europa.eu/eli/dir/2024/1275/oj, May 2024. (Accessed 18 June 2025).

[2] Pittsburgh Corning Europe NV, Environmental product declaration: Foamglas® t3+, https://ibu-epd.com, declaration number: EPD-PCE-20200300-IBB2-EN. Valid until 14-03-2026. (Mar. 2021).

[3] E.A. Yatsenko, B.M. Goltsman, A.I. Izvarin, V.M. Kurdashov, S. Chaudhary, V.A. Smoliy, A.V. Ryabova, L.V. Klimova, N.A. Vilbitskaya, Influence of the temperature field on the formation of thermally foamed silicate materials based on industrial waste, J. Therm. Anal. Calorim. 149 (6) (2024) 2537–2548.

[4] S. Smiljanić, U. Hribar, M. Spreitzer, J. König, Water-glass-assisted foaming in foamed glass production, Ceramics 6 (3) (2023) 1646–1654, https://doi.org/10.3390/ceramics6030101, https://www.mdpi.com/2571-6131/6/3/101.

[5] A. Siddika, A. Hajimohammadi, V. Sahajwalla, A novel eco-friendly foaming technique for developing sustainable glass foams from the waste glass, Resour. Conserv. Recycl. 190 (2023) 106801, https://doi.org/10.1016/j.resconrec.2022.106801, https://www.sciencedirect.com/science/article/pii/S0921344922006334.

[6] Z. Yao, T.-C. Ling, P. Sarker, W. Su, J. Liu, W. Wu, J. Tang, Recycling difficult-to-treat e-waste cathode-ray-tube glass as construction and building materials: a critical review, Renew. Sustain. Energy Rev. 81 (2018) 595–604.

[7] J. Bai, C. Li, Q. Du, C. Dong, Fabrication and properties of self-foamed glass ceramics from red mud and ceramic tile polishing waste, J. Sustain. Metall. 10 (3) (2024) 1559–1571.

[8] P. Boonphayak, S. Khansumled, B. Thavornyutikarn, C. Yatongchai, Waste-to-resource: employing lime mud as a foaming agent in glass foam manufacturing, Constr. Build. Mater. 450 (2024) 138590.

[9] M. Sassi, A. Simon, Waste-to-reuse foam glasses produced from soda-lime-silicate glass, cathode ray tube glass, and aluminium dross, Inorganics 10 (1) (2022), https://doi.org/10.3390/inorganics10010001.

[10] H.R. Fernandes, D.U. Tulyaganov, J.M. Ferreira, Preparation and characterization of foams from sheet glass and fly ash using carbonates as foaming agents, Ceram. Int. 35 (1) (2009) 229–235, https://doi.org/10.1016/j.ceramint.2007.10.019.

[11] H. Zhou, K. Feng, Y. Liu, L. Cai, Preparation and characterization of foamed glass-ceramics based on waste glass and slow-cooled high-titanium blast furnace slag using borax as a flux agent, J. Non-Cryst. Solids 590 (May 2022) 121703, https://doi.org/10.1016/j.jnoncrysol.2022.121703.

[12] S. Deng, C. Li, X. Huang, H. Guo, W. Zhao, B. Yan, P. Li, Insight into the pyrolysis and gas generation behavior of silicomanganese slag and assessing its foaming abilities in foam glass ceramic, J. Clean. Prod. 452 (2024) 142250, https://doi.org/10.1016/j.jclepro.2024.142250, https://www.sciencedirect.com/science/article/pii/S0959652624016986.

[13] H.R. Fernandes, F. Andreola, L. Barbieri, I. Lancellotti, J.M. Pascual, J.M.F. Ferreira, The use of egg shells to produce Cathode Ray Tube (CRT) glass foams, Ceram. Int. 39 (2013) 9071–9078, https://doi.org/10.1016/j.ceramint.2013.05.002.

[14] L.B. Teixeira, V.K. Fernandes, B.G. Maia, S. Arcaro, A.P. de Oliveira, Vitrocrystalline foams produced from glass and oyster shell wastes, Ceram. Int. 43 (2017) 6730–6737, https://doi.org/10.1016/j.ceramint.2017.02.078.

[15] N.P. Stochero, J.O. de Souza Chami, M.T. Souza, E.G. de Moraes, A.P. de Oliveira, Green glass foams from wastes designed for thermal insulation, Waste Biomass Valoriz. 12 (3) (2021) 1609–1620, https://doi.org/10.1007/s12649-020-01120-3.

[16] R.I. Saye, J.A. Sethian, Multiscale modeling of membrane rearrangement, drainage, and rupture in evolving foams, Science 340 (2013) 720–724, https://doi.org/10.1126/science.1230623.

[17] A.E.A. Allen, A. Tkatchenko, Machine learning of material properties: predictive and interpretable multilinear models, Sci. Adv. 8 (18) (2022) eabm7185, https://doi.org/10.1126/sciadv.abm7185, https://www.science.org/doi/abs/10.1126/sciadv.abm7185.

[18] C. Oses, C. Toher, S. Curtarolo, Datadriven design of inorganic materials with the automatic flow framework for materials discovery, Mater. Res. Soc. Bull. 43 (2018), https://doi.org/10.1557/mrs.2018.207.

[19] J. König, A. Lopez-Gil, P. Cimavilla-Roman, M.A. Rodriguez-Perez, R.R. Petersen, M.B. Østergaard, N. Iversen, Y. Yue, M. Spreitzer, Synthesis and properties of open- and closed-porous foamed glass with a low density, Constr. Build. Mater. 247 (2020), https://doi.org/10.1016/j.conbuildmat.2020.118574.

[20] C. Rodrigues, J. König, F. Freire, Prospective life cycle assessment of a novel building system with improved foam glass incorporating high recycled content, Sustain. Prod. Consump. 36 (2023) 161–170.

[21] U. Hribar, M.B. Østergaard, N. Iversen, M. Spreitzer, J. König, The mechanism of glass foaming with water glass, J. Non-Cryst. Solids 600 (2023) 122025, https://doi.org/10.1016/j.jnoncrysol.2022.122025.

[22] K.T. Butler, D.W. Davies, H. Cartwright, O. Isayev, A. Walsh, Machine learning for molecular and materials science, Nature 559 (7715) (2018) 547–555, https://doi.org/10.1038/s41586-018-0337-2.

[23] R. Ramprasad, R. Batra, G. Pilania, A. Mannodi-Kanakkithodi, C. Kim, Machine learning in materials informatics: recent applications and prospects, npj Comput. Mater. 3 (1) (2017) 54, https://doi.org/10.1038/s41524-017-0056-5.

[24] M. Zaki, M. Hasan, L. Pasupulety, K. Kumari, Thermochemistry of manganese oxides in reactive gas atmospheres: probing redox compositions in the decomposition course mno2 → mno, Thermochim. Acta 303 (2) (1997) 171–181, https://doi.org/10.1016/S0040-6031(97)00258-X, https://www.sciencedirect.com/science/article/pii/S004060319700258X.

[25] M. Petković, J. Levatić, D. Kocev, M. Breskvar, S. Džeroski, CLUSplus: a decision tree-based framework for predicting structured outputs, SoftwareX 24 (2023) 101526, https://doi.org/10.1016/j.softx.2023.101526.

[26] L. Breiman, Random forests, Mach. Learn. 45 (2001) 5–32, https://doi.org/10.1023/A:1010933404324.

[27] C.A. Coello Coello, A short tutorial on evolutionary multiobjective optimization, in: International Conference on Evolutionary Multi-Criterion Optimization (LNCS 1993), Springer, Berlin, 2001, pp. 21–40.

[28] E. Zitzler, S. Künzli, Indicator-based selection in multiobjective search, in: Parallel Problem Solving from Nature, PPSN VIII, in: LNCS, vol. 3242, Springer, Berlin, 2004, pp. 832–842.

[29] A. Liefooghe, L. Jourdan, E.G. Talbi, A software framework based on a conceptual unified model for evolutionary multiobjective optimization: ParadisEO-MOEO, Eur. J. Oper. Res. 209 (2011) 104–112, https://doi.org/10.1016/j.ejor.2010.07.023.

[30] U. Hribar, M. Spreitzer, J. König, Applicability of water glass for the transfer of the glass-foaming process from controlled to air atmosphere, J. Clean. Prod. 282 (2021), https://doi.org/10.1016/j.jclepro.2020.125428.

[31] M.B. Østergaard, R.R. Petersen, J. König, Y. Yue, Effect of alkali phosphate content on foaming of CRT panel glass using Mn3O4 and carbon as foaming agents, J. Non-Cryst. Solids 482 (2018) 217–222, https://doi.org/10.1016/j.jnoncrysol.2017.12.041.

[32] M.B. Østergaard, M. Zhang, X. Shen, R.R. Petersen, J. König, P.D. Lee, Y. Yue, B. Cai, High-speed synchrotron X-ray imaging of glass foaming and thermal conductivity simulation, Acta Mater. 189 (2020) 85–92, https://doi.org/10.1016/j.actamat.2020.02.060.

[33] J. König, R.R. Petersen, Y. Yue, D. Suvorov, Gas-releasing reactions in foam-glass formation using carbon and MnxOy as the foaming agents, Ceram. Int. 43 (2017) 4638–4646, https://doi.org/10.1016/j.ceramint.2016.12.133.